Phase-controlled Cooperative Wireless Power Transfer for Backscatter IoT Devices

Jiei Kawasaki, Hikaru Hamase, Kazuhiro Kizaki, Shunsuke Saruwatari, Takashi Watanabe
Graduate School of Information Science and Technology, Osaka University, Japan

***Abstract*—To supply energy for Internet of Things (IoT) devices, this paper proposes phase-controlled wireless power transfer by generating constructive standing waves, on multiple IoT devices, using distributed multiple antennas. The proposed approach realizes equitable power supply distribution among all the IoT devices by switching the phase sets for TX antennas in a time-division manner, and each phase set is optimized for individual IoT devices. In particular, our approach uses received signal strength indicator (RSSI) feedback packets to optimize the phase set of each TX antenna and applies a heuristic algorithm to reduce the number of RSSI feedback packets. We evaluated our approach using computer simulations and experimental micro benchmarks. The computer simulation assumes 64 antennas installed at 2 m intervals on the ceiling of a 15 m by 15 m by 2.5 m room, and each antenna emits 100 dBm continuous non-modulated sine waves. The simulation results show that each of the 10 IoT devices placed on the floor is able to receive an average of approximately 53.6 μW, which is approximately 5.1 times the existing method. The experimental micro benchmarks show the feasibility of the proposed method.**

***Index Terms*—IoT, wireless power transfer, distributed multiple antennas, phase control, backscatter communication**

I. Introduction

Microwave wireless power transfer is suitable for supplying energy to IoT devices or sensors that are placed indoors or inside machines. Although distance attenuation is large and supplied energy is small, the wireless power transfer has at least two merits: stable electric power supply regardless of time and environment, compared to energy harvesting technologies, and the possibility of utilizing wireless access points for data communication. In particular, many researchers in wireless communication are starting to work on the integration of wireless power transmission and information transmission [1]–[10]. We believe that simultaneous wireless information and power transfer (SWIPT) will be a key technology in the IoT era.

This paper addresses the efficiency of wireless power transmission by radio waves while aiming at the future implementation of SWIPT. Wireless power transfer using a single antenna causes an energy shortage problem because an IoT device distant from the antenna obtains less energy. Figure 1 shows an example of power transfer using a single antenna. Some IoT devices may have an energy shortage because of distance attenuation of radio waves.

Using distributed multiple antennas efficiently supplies energy because the relative distance between antennas and IoT devices becomes less than using a single antenna. There are two types of research in wireless power transfer using multiple antennas: one is for a single IoT device [11]–[14] and the other is for multiple IoT devices [15], [16]. Our study focuses on power transfer using multiple antennas for multiple IoT devices.

It is known that the use of distributed multiple antennas for multiple IoT devices causes a standing wave problem [16]. Figure 2 shows an example of the standing wave problem. Constructive and destructive standing waves arise when multiple antennas emit radio waves simultaneously. IoT devices located on destructive standing waves cannot obtain sufficient energy.

To solve the standing wave problem, [16] proposes carrier shift diversity (CSD) power transfer. Figure 3 shows an example of CSD power transfer. CSD power transfer enables uniform energy delivery, in space, by continuously changing the phases of radio waves. The received energy on each IoT device is averaged because the continuous phase change

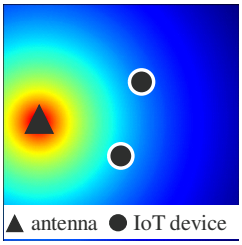

Fig. 1: Single antenna wireless power transfer

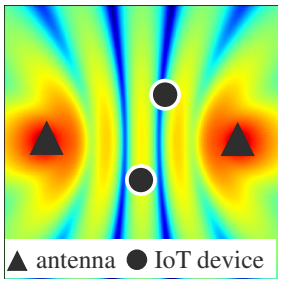

Fig. 2: Distributed multiple antennas power transfer of proposed PC-CPT when $\Theta_1 = \{0, 0\}$

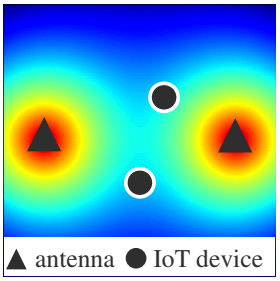

Fig. 3: CSD wireless power transfer

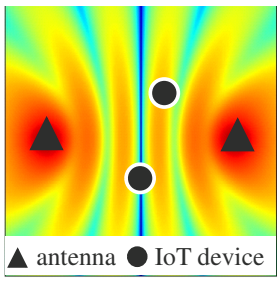

Fig. 4: Proposed PC-CPT when $\Theta_2 = \{\frac{2\pi}{3}, \frac{5\pi}{3}\}$

alternates destructive and constructive interference in a brief period. However, while decreasing the amount of destructive interference, CSD power transfer also decreases the amount of constructive interference.

Therefore this paper proposes phase-controlled cooperative power transfer (PC-CPT). PC-CPT improves power transfer efficiency under the condition of distributed multiple antennas and multiple IoT devices. The proposed PC-CPT controls the phase of emitted radio waves from each antenna to increase the amount of constructive interference at each IoT device. Additionally, switching the phase optimization for individual IoT devices improves the equitable distribution of supplied energy among all IoT devices. Figure 2 and Figure 4 show examples of PC-CPT. The example shows the switching of phase sets Θ_1 and Θ_2, in time-division manner, to change the pattern of constructive interference. We have evaluated the proposed method compared to existing methods, such as CSD, and the evaluation results show the proposed method outperforms existing methods.

The remainder of this paper is organized as follows: Section II introduces the proposed system model which includes a network model and an IoT device model, and shows a received signal strength indicator (RSSI) feedback problem in the model. Section III describes the proposed algorithm to solve the RSSI feedback problem. Section IV discusses the evaluation of the proposed method by computer simulations and experimental micro benchmarks. Finally, Section V concludes the paper.

II. System Model

A. Preliminaries

Figure 5 shows the network model of PC-CPT. Several TX antennas and IoT devices are deployed in a network. The positions of the TX antennas and the IoT devices are fixed. Each TX antenna is connected to a wireless power transmitter and TX antennas transmit the same frequency radio waves while sharing a local oscillator.

The wireless power transmitter controls each phase of the radio wave from each TX antenna by a phase controller. Here the set of phases at all TX antennas is called a phase set $\Theta = \theta_1, \theta_2, \cdots, \theta_m$ where m is the number of TX antennas.

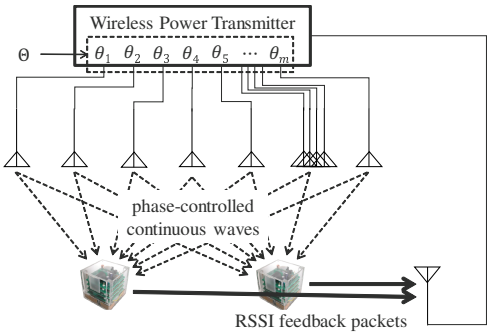

Fig. 5: Network model

TX antennas switch phase sets $\Psi = \Theta_1, \Theta_2, \cdots, \Theta_p$ in time-division manner to supply energy for all IoT devices equitably, where p is the number of phase sets. The wireless power transmitter centrally controls the phase of a radio wave from the TX antenna, according to RSSI feedback from IoT devices.

Figure 6 shows the IoT device model. We assume that each IoT device has a backscatter module, an energy harvest module, and a low power data decoder module. The backscatter module performs data transmission by reflecting and absorbing radio waves from access points. Backscatter communication consumes much less power than conventional wireless communication using an external access point's waves as carrier waves [17]–[19]. The energy harvest module absorbs energy from radio waves, via a rectenna, and stores the energy in a capacitor. The capacitor supplies energy to a main control unit (MCU), a low-power data decoder, and a backscatter module. The data decoder module decodes a data signal from the wireless power transmitter, using very low energy, and an energy detector as described in [20], [21]. Additionally, the IoT device can measure RSSI using the data decoder.

B. RSSI Feedback Problem

In the system model in Section II.A, the optimal power transfer with multiple antennas and IoT devices can be represented as:

minimize

$$\sum_{i=1}^{p} T_i \tag{1}$$

subject to

$$E_j \geq C_j, \forall j \tag{2}$$

$$E_j = \sum_{i=1}^{k} W_{i,j} T_i, \quad \forall j \tag{3}$$

$$W_{i,j} = \mathrm{Energy}(\Theta_i, j) \quad \forall j \tag{4}$$

where k represents the number of phase sets, C_j is the possible stored energy in the capacitor on an IoT device j, and T_i represents transmission duration on phase set i. The equation $W_{i,j} = \mathrm{Energy}(\Theta_i, j)$ represents power supplied to the IoT device j when $\Theta_i = \theta_{i,1}, \theta_{i,2}, \cdots, \theta_{i,m}$ where m is the number of TX antennas. For example, $\theta_{3,5}$ represents a phase

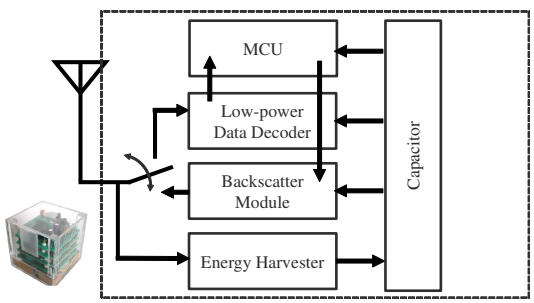

Fig. 6: IoT device model

which is emitted by a 5th TX antenna using a 3rd phase set Θ_3.

The equation (1) is an objective function. The optimal time allocation is the smallest total power transmission duration satisfying the constraint equations (2)–(4). The equation (2) requires that the supplied energy must be smaller than or equal to the possible stored energy of the capacitor on each IoT device. The equation (3) represents the supplied energy at each IoT device. The amount of supplied energy on an IoT device E_j is expressed by the product T_i of the transmission duration of a phase set Θ_i and $W_{i,j}$, which is the amount of power supply per second. The equation (4) represents the amount of power supply per second for each IoT device.

Solving equations (1)–(4) derives optimal power transfer. However, pnr^m, RSSI feedback packets, which indicates the power supplied to an IoT device on a phase set, are a problem. The $\mathrm{Energy}(\Theta_i, j)$ function returns energy supplied to an IoT device j by one RSSI feedback when TX antennas emit a continuous wave using a phase set Θ_i. We need one RSSI feedback packets to acquire the energy supplied to one IoT device. Therefore, we need pnr^m feedback packets to calculate phase sets Ψ because the supplied energy on each phase set must be measured for each IoT device. The number of IoT devices n is usually 128 or 256; r is the resolution of the digital phase controller; and p, which can be infinite, is the number of phase sets.

III. Proposed Approach: Phase-controlled Cooperative Power Transfer

To solve the RSSI feedback problem, this paper proposes phase-controlled cooperative power transfer (PC-CPT). First, PC-CPT reduces the number of feedback packets from infinite to finite by assuming $p = n$. When the number of phase sets is limited to n, a linear programming solver can solve equations (1)–(4). However, we still need n^2r^m RSSI feedback packets when executing $\mathrm{Energy}(\Theta_i, j)$.

To further reduce the number of RSSI feedback packets from n^2r^m to nrm, PC-CPT uses the following:

1) Reduce the number of feedback packets from n^2r^m to nr^m by maximizing the power supplied to only one IoT device per phase set.
2) Reduce the number of feedback packets from nr^m to nrm by sequentially determining each phase from AP 1 to AP m when estimating the phase set which maximizes the power supplied to an IoT device.
3) Calculate the duration of transmission on each phase set using the approximate reciprocal ratio of the supplied power of each IoT device.
4) Calculate the approximate reciprocal ratio using one RSSI feedback per phase set.

Algorithm 1 shows how to estimate phase sets. In the **Algorithm 1**, i, j, k are variables for iteration, t and a are temporary variables, n is the number of IoT devices, m is the number of TX antennas, r is the resolution of the digital phase controller, $\mathrm{startRF}(j, k)$ is a function that lets a TX antenna j start emitting a continuous wave on setting k to the digital phase controller, $\mathrm{stopRF}(j)$ is a function such that TX antenna j stops emitting a continuous wave, $\mathrm{getRSSI}(i)$ is a function that gets RSSI feedback from IoT device i, and $\mathrm{stopAllRF}()$ is a function that stops all TX antennas' emissions of a continuous wave.

Algorithm 1 Phases estimation

```
1:  for i = 1 to n do
2:    startRF(1, 0)
3:    for j = 2 to m do
4:      a ⇐ 0
5:      for l = 0 to r − 1 do
6:        ψ ⇐ 2π l/(r−1)
7:        startRF(j, ψ)
8:        t ⇐ getRSSI(i)
9:        if a < t then
10:         a ⇐ t
11:         θ_{i,j} ⇐ ψ
12:       end if
13:       stopRF(j)
14:     end for
15:     startRF(j, θ_{i,j})
16:   end for
17:   stopAllRF()
18: end for
```

Algorithm 1 estimates n phase sets for each IoT device sequentially. In lines 1–2 of **Algorithm 1**, TX antenna 1 starts emitting a continuous wave, with phase 0, when estimating the phase set of the sensor i. Next, **Algorithm 1** controls the phases of signals from TX antenna 2 to m for IoT device i. In lines 3–12 of **Algorithm 1**, the phase, which maximizes the received power of IoT device i of a signal from TX antenna j, is estimated by acquiring RSSI feedback from IoT device i. In line 14 of **Algorithm 1**, after estimating the phase of the signal from TX antenna j, the TX antenna j starts emitting a continuous wave with the estimated phase. In line 16 of **Algorithm 1**, all TX antennas stop emission of a continuous wave after all phases of the signals from TX antennas for the IoT device i are estimated.

The ratio of the duration of transmission R_i, using a phase set i and the entire transmission time, is determined by:

$$R_i = \frac{T_i}{\sum_{j=1}^{n} T_j}, \quad \forall i$$
$$T_i = \frac{\sum_{j=1}^{n} W_{j,j}}{W_{i,i}}, \quad \forall i. \tag{5}$$

TX antennas deliver energy to each IoT device uniformly by calculating the power transmission duration of each phase set as the approximate reciprocal ratio of each supplied power. As can be seen in equation (5), the approximate reciprocal ratio only uses each supplied power $W_{a,b}$, where $a = b$, to reduce the number of RSSI feedback packets.

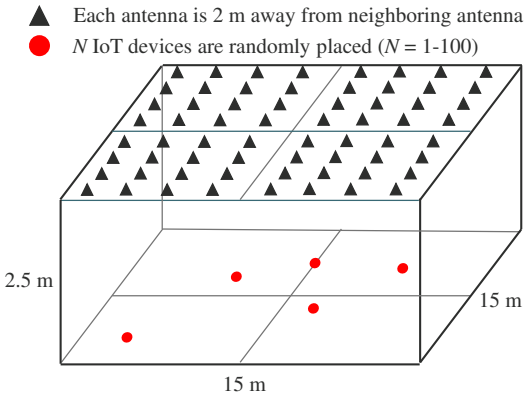

Fig. 7: Environmental settings

IV. Evaluation

We evaluated the proposed method using computer simulations and experimental micro benchmarks:

A. Computer Simulations

1) Evaluation settings: Figure 7 shows environmental settings. We assume that the TX antennas are embedded in the ceiling lights, and the room size is 15 m by 15 m by 2.5 m. There are 64 TX antennas and each antenna is 2 m away from a neighboring antenna. Each antenna transmits a 10-mW continuous non-modulated sine wave at 2.4 GHz, and the path loss is assumed to follow the Friis equation. The number of IoT devices varies from 1 to 100 and the position of the IoT devices are random.

To evaluate the proposed PC-CPT we compare the following three methods:

1) uncontrolled power transmission (no control),
2) carrier shift diversity (CSD) [16], and
3) PC-CPT (proposed).

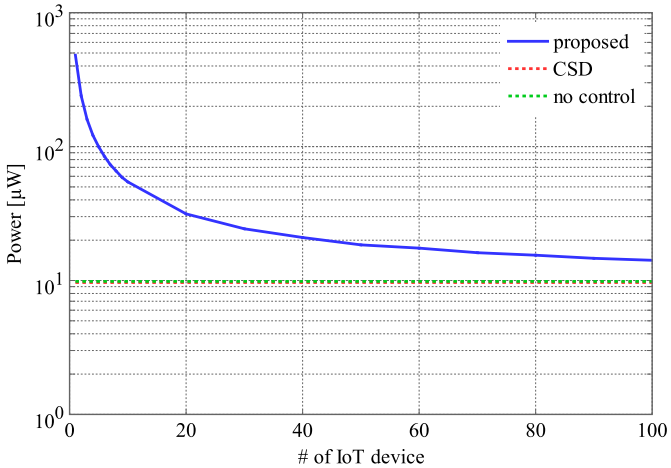

Fig. 8: Average received power

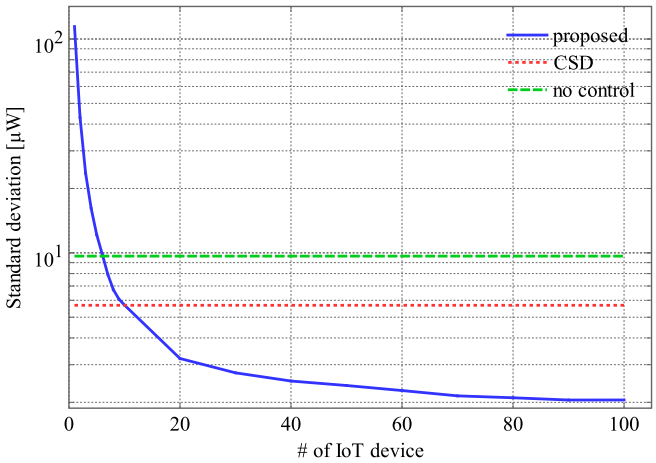

Fig. 9: Standard deviation

2) Average Received Power: We evaluated average received power per IoT device, without changing the number of IoT devices in a network. The received power is the average of 100 trials. Figure 8 shows the evaluation result. The horizontal axis denotes the number of IoT devices and the vertical axis denotes the average received power from each IoT device. As shown in Figure 8, the proposed approach outperforms other methods, especially when the number of IoT devices is small. For example, when the number of IoT devices equals 1, 10 or 100, the average received power is approximately 481.4 μW, 54.5 μW, and 14.2 μW, which are approximately 49.8 times, 5.6 times, and 1.5 times the performance of CSD, respectively. As the number of IoT devices increases, the difference between the proposed method and the existing method becomes smaller.

3) Fairness: To evaluate the fairness of the proposed approach, we evaluated the standard deviation of the received power of IoT devices while changing the number of IoT devices. Figure 9 shows the evaluation result. The horizontal axis denotes the number of IoT devices, and the vertical axis denotes the standard deviation of received power for each IoT device. In Figure 9, smaller standard deviations correspond to higher performances. As shown in Figure 9, the proposed approach realizes higher fairness when the number of IoT devices is large. For example, when the number of IoT devices is 100, the standard deviation of received power is about 2.1 μW, which is about 40 percent of CSD. When the number of IoT devices is small, the standard deviation of the proposed approach is higher than CSD's, because the proposed approach delivers much higher energy compared to CSD, and there is no control as described in Section IV-A2. For example, when the number of IoT devices equals 1 or 10, the standard deviations of received power are about 114.3 μW and 5.9 μW, which are 21.2 times and 1.1 times the standard deviations of CSD, respectively.

To understand the relation between the average received power and the fairness in detail, we evaluated the cumulative distribution function of the received power per IoT device in

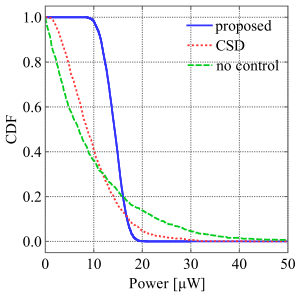

Fig. 10: Cumulative distribution function over the received power when $N = 100$

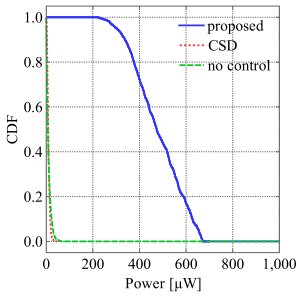

Fig. 11: Cumulative distribution function of the received power when $N = 1$

all trials. Figure 10 shows the cumulative distribution function versus received power when the number of IoT devices is 100. As shown in Figure 10, the proposed method achieves the highest received power. In particular, 100 % of the IoT devices receive power greater than about 8.4 μW and there is a quick drop-off above that point. We can also see CSD has higher received power than with no control and has a steeper drop-off than with no control.

Figure 11 shows the cumulative distribution function of the received power when the number of IoT devices is 1. In Figure 11, the drop-off is gentler than CSD's with no control, because the standard deviation of the proposed method is much larger than CSD with no control, when the number of IoT devices is 1, as described above in Figure 9. However, Figure 11 shows that the received power is much higher than CSD's with no control.

B. Experimental Micro Benchmarks

To verify the feasibility of the proposed method, we have conducted experimental micro benchmarks. Figure 12 shows an experimental configuration. There are four TX antennas and three RX antennas as IoT devices. TX antennas and RX antennas are Inventek Systems W24-SSMA-M which is a monopole antenna whose gain is 2.15 dBi. In this paper, we represent the transmitting antenna i as TXi and the receiving antenna i as RXi. The four TX antennas are connected to a 2.4 GHz non-modulated sine wave transmitting Texas Instruments CC2531 through a phase shifter Analog Device, HMC928 LP5E, for each TX antenna. Each phase shifter is controlled by an Atmel ATMEGA128L-8MU MCU, connected to a Panasonic Let's Note CF-SZ6 laptop through a USB with a Future Technology Devices International (FTDI) FT245RL. The transmission power from each antenna is approximately 25 μW because the transmission power of the transmitter is 1 mW, and the transmit signal is divided between 4 antennas, and the power loss of each phase shifter is approximately 10 dB. Each RX antenna is connected to a power sensor, Analog Device LT5534, and the output analog voltage of the power sensor is converted to a digital value using an AD converter on Silicon Labs C8051F360 MCUs. The three MCUs are connected to a PC, through a USB, with an FTDI FT232HL.

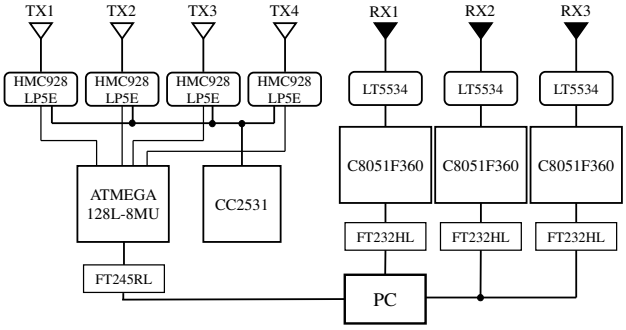

Fig. 12: Experimental device

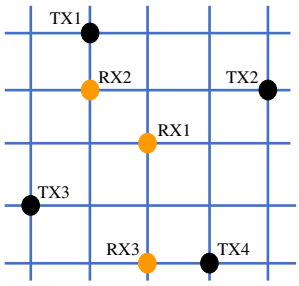

Fig. 13: Placement A

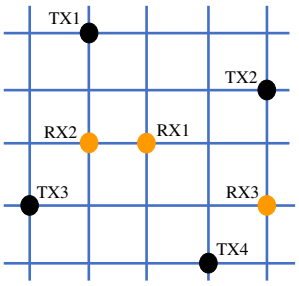

Fig. 14: Placement B

A PC processes the proposed PC-CPT described in Section III. We measured results in an anechoic chamber to cut off external radio waves.

Figure 13 and Figure 14 show the layout of the TX and RX antennas. Four TX antennas and three RX antennas were placed on the 5×5 grid. Each grid size is 12.5 cm. The TX antennas are placed in a 39.5 cm by 39.5 cm square. Figure 13 and Figure 14 show placement A and placement B, respectively. The RX antennas are placed according to the following criteria: First, RX1 is placed in the center of the grid, which is equidistant from the TX antennas. The position of RX1 is fixed in all experiments for reference to other RX antennas throughout the experiments. And second, RX2 is placed inside the square surrounded by the TX antennas. RX2 is placed adjacent to a TX antenna and that placement is susceptible to interference from other TX antennas. And third, RX3 is placed outside the square surrounded by the TX antennas. RX3 is placed adjacent to a TX antenna and that placement is less susceptible to interference as compared to RX2.

Table I and Table II list the experimental results of placement A and placement B. From Table I and Table II, we can see the following two things: First, the proposed CP-CPT outperforms CSD in both placements A and B. In placement A, the proposed CP-CPT has about 1.7 times higher performance than CSD because the average received powers of the proposed CP-CPT and CSD are 37.5 and 21.6, respectively. In placement B, the proposed CP-CPT also has about 1.7 times higher performance than CSD based on average received powers of the proposed CP-CPT and CSD of 30.5 and 18.3, respectively.

TABLE I: Received power, transmission time ratio, and standard deviation in placement A

	RX1	RX2	RX3	R_i	σ
Θ_1	66.7 nW	29.9 nW	22.1 nW	0.39	19.4 nW
Θ_2	6.8 nW	151.2 nW	1.3 nW	0.17	69.4 nW
Θ_3	8.5 nW	14.3 nW	59.3 nW	0.44	22.7 nW
proposed	33.9 nW	43.9 nW	34.8 nW	N/A	4.5 nW
CSD	13.1 nW	35.8 nW	15.9 nW	N/A	10.1 nW

TABLE II: Received power, transmission time ratio, and standard deviation in placement B

	RX1	RX2	RX3	R_i	σ
Θ_1	83.4 nW	0.1 nW	3.8 nW	0.22	38.4 nW
Θ_2	5.1 nW	118.4 nW	11.5 nW	0.16	60.0 nW
Θ_3	10.6 nW	40.8 nW	30.2 nW	0.62	12.5 nW
proposed	25.7 nW	44.3 nW	21.4 nW	N/A	9.9 nW
CSD	17.5 nW	28.7 nW	8.7 nW	N/A	8.2 nW

And second, the proposed CP-CPT does not always achieve higher fairness than CSD: CP-CPT has a smaller standard deviation than CSD in placement A, but CP-CPT has a larger standard deviation than CSD in placement B. The reason why the proposed CP-CPT sometimes has a larger standard deviation is related to equation (5). The proposed CP-CPT only uses $W_{a,b}$, where $a = b$, to calculate R_i with reducing the number of RSSI feedback packets. It is desirable to calculate R_i using the received power at all antennas for all phase sets. For example, in Table II, R_2 should be smaller because the received power of RX2 is larger when the phase set is Θ_3.

V. Conclusion

Here we have proposed a phase-controlled cooperative power transmission with distributed multiple antennas for multiple IoT devices. The key ideas of our approach are RSSI feedback-based phase control and a heuristic feedback reduction algorithm. We have evaluated our approach by computer simulations and experimental micro benchmarks. The evaluation shows our approach is better than existing methods such as CSD and an uncontrolled approach.

Acknowledgment

We acknowledge the support received by JSPS Science Research Grants (JP16H01718, JP17J02859, JP17KT0042, and JP16K16044) and the NTT Access Network Service Laboratories and Panasonic Corporation.

References

[1] T. D. P. Perera, D. N. K. Jayakody, K. S. Shree, S. Chatzinotas, and J. Li, "Simultaneous wireless information and power transfer (SWIPT): Recent advances and future challenges," *IEEE Communications Surveys Tutorials*, vol. 20, no. 1, pp. 264–302, 2018.

[2] K. Yamazaki, Y. Sugiyama, Y. Kawahara, S. Saruwatari, and T. Watanabe, "Preliminary evaluation of simultaneous data and power transmission in the same frequency channel," in *2015 IEEE Wireless Communications and Networking Conference (IEEE WCNC'15)*, March 2015, pp. 1237–1242.

[3] C. Psomas and I. Krikidis, "Adaptive variable-length feedback using wireless power transfer for opportunistic beamforming," in *Proceedings of 2016 IEEE International Conference on Communications (IEEE ICC'16)*, May 2016, pp. 1–6.

[4] B. Luo, P. L. Yeoh, R. Schober, and B. S. Krongold, "Optimal energy beamforming for distributed wireless power transfer over frequency-selective channels," in *Proceedings of 2019 IEEE International Conference on Communications (IEEE ICC'19)*, May 2019, pp. 1–6.

[5] H. Kassab and J. Louveaux, "Simultaneous wireless information and power transfer using rectangular pulse and CP-OFDM," in *Proceedings of 2019 IEEE International Conference on Communications (IEEE ICC'19)*, May 2019, pp. 1–6.

[6] D. K. P. Asiedu, S. Mahama, S. W. Jeon, and K. jae Lees, "Joint optimization of multiple-relay amplify-and-forward systems based on simultaneous wireless information and power transfer," in *Proceedings of 2018 IEEE International Conference on Communications (IEEE ICC'18)*, May 2018, pp. 1–6.

[7] W. Qu, X. Cheng, M. Zhang, and C. Chen, "Spatial-modulation based wireless information and power transfer with full duplex relaying," in *Proceedings 2018 IEEE International Conference on Communications (IEEE ICC'18)*, May 2018, pp. 1–6.

[8] M. Mohammadi, B. K. Chalise, H. A. Suraweera, and Z. Ding, "Wireless information and power transfer in full-duplex systems with massive antenna arrays," in *Proceedings of 2017 IEEE International Conference on Communications (IEEE ICC'17)*, May 2017, pp. 1–6.

[9] O. L. A. Lopez, R. D. Souza, H. Alves, and E. M. G. Fernandez, "Ultra reliable short message relaying with wireless power transfer," in *Proceedings of 2017 IEEE International Conference on Communications (IEEE ICC'17)*, May 2017, pp. 1–6.

[10] A. A. Okandeji, M. R. A. Khandaker, and K. K. Wong, "Wireless information and power transfer in full-duplex communication systems," in *Proceedings of 2016 IEEE International Conference on Communications (IEEE ICC'16)*, May 2016, pp. 1–6.

[11] D. W. K. Ng and R. Schober, "Secure and green SWIPT in distributed antenna networks with limited backhaul capacity," *IEEE Transactions on Wireless Communications*, vol. 14, no. 9, pp. 5082–5097, 2015.

[12] S. Lee and R. Zhang, "Distributed wireless power transfer with energy feedback," *IEEE Transactions on Signal Processing*, vol. 65, no. 7, pp. 1685–1699, 2017.

[13] X. Fan, H. Ding, S. Li, M. Sanzari, Y. Zhang, W. Trappe, Z. Han, and R. E. Howard, "Energy-ball: Wireless power transfer for batteryless internet of things through distributed beamforming," *Proceedings of the ACM on Interactive, Mobile, Wearable and Ubiquitous Technologies*, vol. 2, no. 2, pp. 65:1–65:22, June 2018.

[14] K. W. Choi, A. A. Aziz, D. Setiawan, N. M. Tran, L. Ginting, and D. I. Kim, "Distributed wireless power transfer system for internet-of-things devices," *IEEE Internet of Things Journal*, 2018.

[15] M. Y. Naderi, P. Nintanavongsa, and K. R. Chowdhury, "RF-MAC: A medium access control protocol for re-chargeable sensor networks powered by wireless energy harvesting," *IEEE Transactions on Wireless Communications*, vol. 13, no. 7, pp. 3926–3937, 2014.

[16] D. Maehara, G. K. Tran, K. Sakaguchi, K. Araki, and M. Furukawa, "Experiments validating the effectiveness of multi-point wireless energy transmission with carrier shift diversity," *IEICE Transactions on Communications*, vol. 97, no. 9, pp. 1928–1937, 2014.

[17] B. Kellogg, V. Talla, S. Gollakota, and J. R. Smith, "Passive Wi-Fi: Bringing low power to Wi-Fi transmissions," in *Proceedings of 13th USENIX Symposium on Networked Systems Design and Implementation (USENIX NSDI'16)*, vol. 16, 2016, pp. 151–164.

[18] N. V. Huynh, D. T. Hoang, X. Lu, D. Niyato, P. Wang, and D. I. Kim, "Ambient backscatter communications: A contemporary survey," *IEEE Communications Surveys & Tutorials*, vol. 20, no. 4, pp. 2889–2922, May 2018.

[19] T. Higashino, A. Uchiyama, S. Saruwatari, H. Yamaguchi, and T. Watanabe, "Context recognition of humans and objects by distributed zero-energy IoT devices," in *Proceedings of The 39th IEEE International Conference on Distributed Computing Systems (IEEE ICDCS'19)*, July 2019, pp. 1–7.

[20] B. Kellogg, A. Parks, S. Gollakota, J. R. Smith, and D. Wetherall, "Wi-fi backscatter: Internet connectivity for RF-powered devices," in *Proceedings of the 2014 ACM conference on SIGCOMM (ACM SIGCOMM'14)*, August 2014, pp. 607–618.

[21] B. Kellogg, V. Talla, and S. Gollakota, "Bringing gesture recognition to all devices," in *Proceedings of 11th USENIX Symposium on Networked Systems Design and Implementation (USENIX NSDI'14)*, April 2014, pp. 303–316.